Performance Analysis of LTE Random Access Protocol With an Energy Harvesting M2M Scenario

Sina Khoshabi Nobar, Mohamed Hossam Ahmed, *Senior Member, IEEE*, Yasser Morgan, *Member, IEEE*, and Samy A. Mahmoud, *Life Senior Member, IEEE*

***Abstract*—In this article, we analyze the performance of the long-term evolution random access procedure with the Third Generation Partnership Project's access class barring (ACB) mechanism in an energy harvesting (EH) machine-to-machine (M2M) scenario. To circumvent the state-space explosion in the conventional Markov-chain-based analysis due to time-dependent traffic pattern and data and energy buffer status, we develop an analytical model that combines mean-value analysis with the Markov-based analysis. Based on the analytical model, the random access success probability, the access delay of the network, and the average time duration between two successive successful transmissions are derived. Our analysis suggests that in the EH scenario, despite the lower number of the contending nodes in comparison with the non-EH scenario, the ACB parameters must be chosen in a more conservative way to avoid excessive collisions. The ACB parameters include access barring rate and mean barring duration. We also study an energy threshold-based activation policy and investigate the joint effects of this policy and the ACB mechanism on the random access success probability. The extensive simulations were conducted to evaluate the accuracy of the analytical model.**

***Index Terms*—Energy harvesting (EH), Internet of Things (IoT), long-term evolution (LTE), machine-to-machine (M2M), network performance analysis.**

I. Introduction

THE implementation of the future Internet of Things (IoT) systems relies on the presence of enabling the networking technology and machine-to-machine (M2M) communication protocol. Due to their pervasiveness, cellular networks are considered as the natural candidates to serve as a platform for IoT systems and to facilitate M2M communication. However, the random access channel of the long-term evolution (LTE) and LTE-advanced (LTE-A) cellular networks are not suited for M2M communications [1]. This is due to the fact that they are designed to handle human-to-human (H2H) data traffic where a relatively low number of user devices initiate random access procedure to access the network, while, in M2M communication, a massive number of devices contend for accessing the network simultaneously, leading to significant performance degradation. The Third Generation Partnership Project (3GPP) recognized this problem and proposed two solutions to deal with it [2]. The first solution is called access class barring (ACB), and the second solution is called extended access barring (EAB). The performance of the LTE network with the ACB and EAB schemes has been examined in [3]–[5], while the results for the bursty LTE random access can be found in [6].

The performance analysis and optimization of the random access procedure of LTE standard in the M2M scenario have been analyzed in [7], where different enhancement methods were presented. For example, the authors in [8] proposed a joint access control and resource allocation for M2M communication in the LTE network, where the access probability and the number of random access opportunities are optimized. A two-stage random access approach is proposed in [9] to decrease the wasting uplink resources. A method based on successive interference cancellation is proposed in [10] to resolve the collision in the random access procedure of LTE in the massive M2M scenario. Lin *et al.* [11] proposed preallocation-based random access to deal with a large number of simultaneous access requests. A modification in the four-step random access procedure of LTE is proposed in [12] to provide a more efficient access method for M2M devices by reducing the required steps. A survey of random access protocols for M2M communication over the LTE network is available in [13].

Another enabler for IoT is the energy harvesting (EH) technology which provides a considerably long lifetime for the devices and eliminates the need for frequent battery replacement. There are few published articles that examined the performance of the random access protocol of LTE from the point of view of EH and consumption. A simulation-based study on the performance of the random access channel of the LTE network in the M2M scenario from the energy perspective is presented in [14]. Shih *et al.* [15] introduced a threshold-based activation policy for the EH legacy LTE network. That work was subsequently extended to study user-initiated and eNB-initiated access mechanism in the EH legacy LTE network through simulation, without considering M2M-specific access control mechanisms, such as EAB or ACB [16].

Manuscript received July 9, 2019; revised August 27, 2019 and September 18, 2019; accepted October 1, 2019. Date of publication October 8, 2019; date of current version February 11, 2020. This work was supported in part by NSERC (Canada) under Discovery Grant 2014-03638 and Grant 2018-20301. *(Corresponding author: Samy A. Mahmoud.)*

S. Khoshabi Nobar and S. A. Mahmoud are with the Department of Systems and Computer Engineering, Carleton University, Ottawa, ON K1S 5B6, Canada (e-mail: sina.khoshabinobar@carleton.ca; mahmoud@sce.carleton.ca).

M. H. Ahmed is with the Faculty of Engineering and Applied Science, Memorial University of Newfoundland, St. John's, NL A1B 3X5, Canada (e-mail: mhahmed@mun.ca).

Y. Morgan is with the Faculty of Engineering and Applied Science, University of Regina, Regina, SK S4S 0A2, Canada (e-mail: yasser.morgan@uregina.ca).

Digital Object Identifier 10.1109/JIOT.2019.2946295

However, to the best of our knowledge, no research work has been published previously to analyze the performance of the random access channel of LTE in the EH-M2M scenario, where the joint effects of the EH and the ACB mechanism were analytically studied.

A number of published research papers have presented approaches in networks other than LTE for the design of medium access control (MAC) protocols in the EH networks with M2M communication. For example, an MAC protocol based on energy-level-related priorities was introduced and optimized in [17]. The performance of time-division multiple access (TDMA) and nonorthogonal multiple access (NOMA) are analyzed and compared in [18] for the EH scenario. Vázquez-Gallego *et al.* [19], [20] introduced an EH-aware contention-tree-based access protocol, where the theoretical performance metrics, such as probability of delivery, are derived. The probability of delivery for dynamic frame slotted-ALOHA protocol under the EH scenario with and without reservation was investigated in [21] and [22].

The goal of the work presented in this article is to analyze the existing random access protocol of LTE, augmented with the 3GPP's ACB mechanism to accommodate the massive number of user equipment (UE) involving M2M communication in which the devices are powered by EH sources. The approach followed in addressing this problem is based on developing a recursive equation to formulate the transient number of the contending UEs during a cycle and capture the joint effects of the ACB mechanism and energy availability. A Markov chain model for the battery of the UEs is then constructed to capture the interdependency between data transmission and energy availability. The combination of introduced recursive equation and the Markov chain enable us to analyze the performance of the random access protocol of the LTE network with the ACB mechanism in the EH scenario in terms of random access success probability (or normalized throughput[1]), delay, and the average duration between two successive transmissions by a UE that are also successful. In addition, we study the joint effects of an energy-threshold-based activation policy and the ACB mechanism on the performance of the random access procedure. The analytical results are presented and validated using the computer simulations. As an added benefit, the analysis and simulation works enable the determination of the optimal values of the ACB parameters for both EH and non-EH cases.

It is worth noting that an alternative to the approach adopted and presented in this article would be to model the entire system using a conventional Markov chain. In this alternative approach, a 4-D Markov chain will have to be constructed to include the following four state indicators: 1) random access opportunity (RAO) index (time index); 2) data buffer state; 3) access barring state; and 4) energy state. The resultant state-space will thus be enormous and analytically intractable. The complexity of the alternative approach provides further justification for the method presented in this article which is shown to be both computationally and analytically manageable.

The remaining sections of this article are organized as follows. Section II presents the EH and consumption models, as well as the random access procedure of the LTE protocol with 3GPP's ACB mechanism. The analytical model to characterize the performance of the network is presented in Section III, while the threshold-based activation policy is discussed in Section IV. The derived analytical model is evaluated using the simulation in Section V along with discussions regarding the optimal design of the ACB parameters. Finally, Section VI provides a summary for the conclusions of this article.

II. System Model

We consider an LTE network with N M2M devices, also called UEs, which are inside the coverage area of a single evolved-node B (eNB), and trying to access the network resources. The network operates in the random access mode rather than the scheduled access mode.

A. Temporal Structure and Data Traffic Model

We assume that the time axis is divided into cycles with a duration of t_C seconds. Each UE generates a single packet during a portion of a cycle, t_P ($t_P < t_C$), and the packet arrival time follows a general probability distribution function (PDF), $p_A(t)$ for $0 \leq t \leq t_P$. This data traffic model corresponds to the semi-periodic monitoring applications, where the M2M device has to report an observation result in each cycle and is used by 3GPP to evaluate the M2M scenario in [23], as well as in [3], [4], and [24]. Since each node only generates a single packet during a cycle, and the generation time of that packet is randomly distributed according to $p_A(t)$, the data traffic model is classified as a random unsaturated arrival model. Furthermore, if a packet is not transmitted until the end of the cycle (due to the ACB or backoff mechanisms), it will be discarded, since the UE will generate a new packet with fresh data in the next cycle.

B. Energy Model

Each UE has an EH unit that harvests energy during the cycle and injects the harvested energy into the battery of the UE at the end of the cycle. Let E denotes the available energy at the battery of a typical UE in the beginning of a cycle, and E_h denotes the random amount of the harvested energy during a cycle. The harvested energy during a cycle is available for use at the beginning of the next cycle. Following the work in [20], we consider a discrete EH model in which E_h is a discrete random variable with arbitrary probability mass function (PMF), with the mean value of e_h. For instance, E_h can be modeled by Poisson and compound Poisson random variables, if the EH sources are piezoelectric [25] and solar [26], respectively. The general probabilistic model also includes the deterministic EH case when the coherence time of the EH process is much larger than the duration of the entire communication session [27]. The random variable E_h is independent and identically distributed over cycles and devices. On the

[1]In this article, we use the terms "normalized throughput," "throughput," and "random access success probability," interchangeably. In fact, the success probability of the random access procedure can be converted into the unit of bits per second, considering the expected data packet size and cycle duration.

other hand, the amount of the consumed energy in a successful and collided access attempts are E_s and E_c energy units, respectively. Note that E_s includes the subsequent energy consumption in the signaling and data packet transmission, in addition to the consumed energy during the random access procedure. Therefore, in general, $E_s \geq E_c$. According to the discrete EH and consumption models, we assume that E_h, E_s, and E_c are the integer multiples of an energy unit. Otherwise, we can rescale the energy unit to satisfy this assumption.

A UE is active during a cycle if it has the energy required for at least one successful transmission. Otherwise, it keeps silent until the beginning of the next cycle, while it performs EH. The probability of a typical UE to have the energy required for r collided access attempts and a successful transmission, $p_{ea}(r)$ is given by

$$p_{ea}(r) = \begin{cases} \mathbb{P}(rE_c + E_s \leq E < (r+1)E_c + E_s) & 0 \leq r < N_{\mathrm{PTmax}} - 1 \\ \mathbb{P}(rE_c + E_s \leq E) & r = N_{\mathrm{PTmax}} - 1 \end{cases} \quad (1)$$

where N_{PTmax} is the maximum number of access attempts defined by the standard. We obtain the value of $p_{ea}(r)$ in the next section.

C. Random Access Procedure

The LTE random access procedure proposed by the 3GPP [2] for the M2M scenario is illustrated in Fig. 1. The flowchart in Fig. 1 is for the case when the channel effect is ignored and concurrent transmission of a preamble by two or more UEs definitely results in decoding errors in the eNB. The study of the complete four-step random access procedure under the imperfect physical channels and the advanced features like power ramping capability is considered as our future works. Under our assumptions, the random access procedure can be divided into two phases, as described in the following.

1) *The ACB Phase:* The goal of the ACB scheme is to reshape the traffic pattern and redistribute the packet arrivals such that the number of concurrent access attempts and, hence, collisions are reduced. Two parameters characterize the ACB scheme, p_{acb} and t_{acb}, which are broadcast by the eNB through *SystemInformationBlockType2* (SIB2) message. The parameter p_{acb} is the access barring rate while t_{acb} is the mean barring duration (in seconds). Each UE generates a random number between zero and one, and if the number is less than p_{acb} it is allowed to proceed to the second phase, otherwise, it is barred from contention for a random time that is chosen uniformly between $0.7t_{\mathrm{acb}}$ and $1.3t_{\mathrm{acb}}$, with a mean of t_{acb}.
2) *The LTE Random Access Phase:* After completing the first phase, a UE follows the random access procedure of legacy LTE in which it randomly selects one of the R available orthogonal preambles and transmits it through physical random access channel (PRACH) to the eNB. In LTE, the time is divided into frames, each with a duration of 10 ms and further subframes, with a duration of 1 ms. A UE is allowed to send a preamble only in specific subframes called RAO. The number of RAOs in a frame is determined by *prach-ConfigIndex*, which is broadcast by the eNB. Similar to the analysis provided in [4], we assume that the eNB can successfully decode a preamble if it is transmitted only by one UE. Upon transmitting a preamble, the UE waits for w_r (7 ms) to receive random access response (RAR), where w_r consists of preamble processing time by the eNB and the duration of an RAR window. Note that because of the limited number of uplink grants in an RAR message, the eNB can only accept up to a predefined maximum number of access requests, N_{UL}, per RAR window. If the UE does not receive an RAR, the backoff counter begins, i.e., the UE waits for a random time which is chosen uniformly between 0 and w_{bo}, with a mean of $(w_{bo}/2)$, before retrying access, where w_{bo} is defined as the backoff window as in Table I.

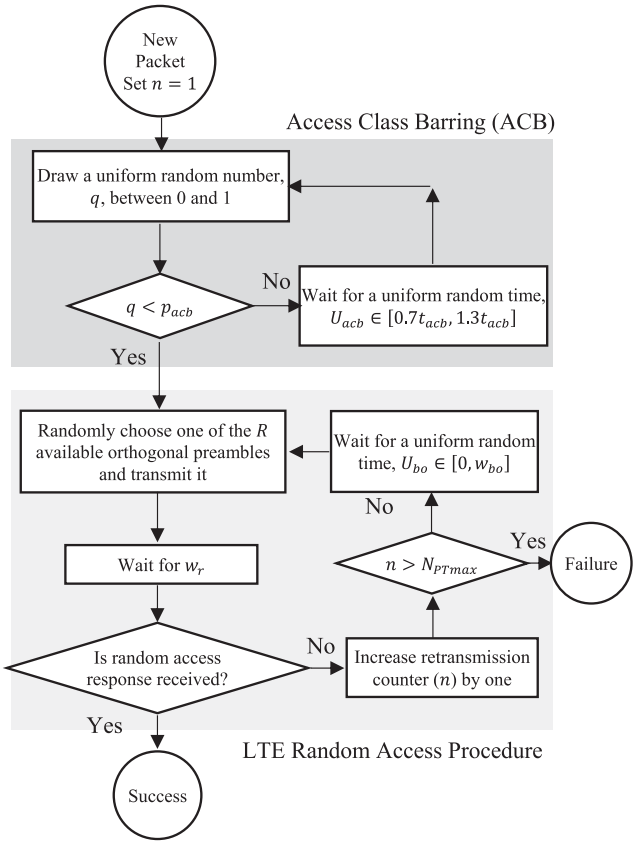

Fig. 1. Random access procedure executed by each UE, assuming an ideal physical channel.

Since any random-access-related action only takes place in RAO, we change the unit of time from "second" to "RAO," where each RAO is t_{rao} seconds that is determined according to *prach-ConfigIndex*. For any time-related parameter, lowercase and capital letters (e.g., w_r and W_r) refer to the value of the parameter in the unit of second and RAO, respectively. While we previously defined $p_A(t)$ as the PDF of packet arrival time, we define $p_A(i)$ as the PMF of packet arrival time, where i refers to the ith RAO in a cycle.

Accordingly, considering the uniform distribution of the barring and backoff times, it is necessary to transform these

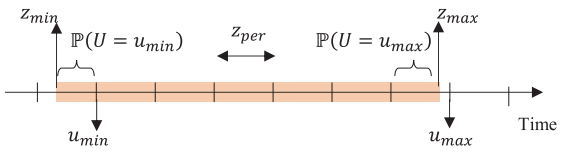

Fig. 2. Transforming continuous uniform distribution into discrete equivalent.

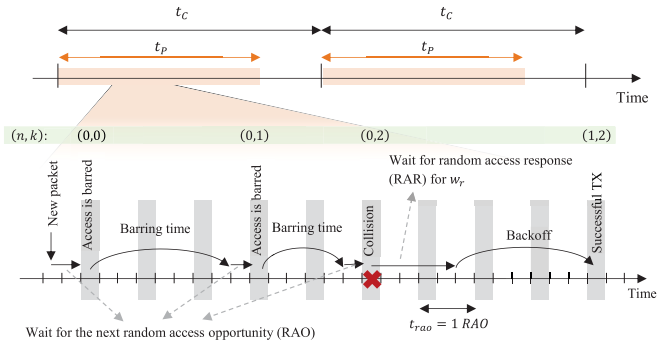

Fig. 3. Sample timeline for an active UE.

continuous distributions into the discrete equivalents with RAO being the discrete unit of the time axis.

Remark 1: Suppose we have a continuous uniform random variable, Z, that is defined between $z_{\min}$ and $z_{\max}$ seconds on the time axis. Also, suppose there are equally spaced points on the time axis. The distance between two adjacent points is z_{per} seconds. We define U as a discrete random variable with $U = \lceil (Z/z_{\text{per}}) \rceil$, that takes integer values in the range $[u_{\min} = \lceil (z_{\min}/z_{\text{per}}) \rceil, u_{\max} = \lceil (z_{\max}/z_{\text{per}}) \rceil]$. We are interested in the PMF of U, i.e., $\mathbb{P}(U = u)$. According to Fig. 2, the probabilities of choosing the boundary points are given by

$$\mathbb{P}(U = u_{\min}) = \frac{u_{\min} z_{\text{per}} - z_{\min}}{z_{\max} - z_{\min}}$$
$$\mathbb{P}(U = u_{\max}) = \frac{z_{\max} - (u_{\max} - 1) z_{\text{per}}}{z_{\max} - z_{\min}} \tag{2}$$

and the probability of choosing any other point, u, between $u_{\min}$ and $u_{\max}$ is

$$\mathbb{P}(U = u) = \frac{z_{\text{per}}}{z_{\max} - z_{\min}}. \tag{3}$$

This result is used in the next section.

A sample timeline for the network is presented in Fig. 3, where the gray-shaded subframes are RAOs. A more comprehensive discussion on the random access procedure of LTE can be found in [1]. Most of the notations used in this article are summarized in Table I.

III. Performance Analysis

In this section, we derive expressions for the energy consumption, throughput, and delay of the network. It is important, however, to note that the collision probability in each RAO depends on the number of contending UEs in that particular RAO. Therefore, as the first step, we derive the number of UEs that are trying to access the PRACH in any given RAO. Our approach to this end is to separate the UEs based on their initial energy and their random access status, which makes it possible to study the evolution of the number of contending UEs over time, even when the packet arrivals follow a time-variant pattern rather than the conventional Markovian pattern.

TABLE I
Summary of Notations

Symbol	Meaning	Numerical Value
E	Random variable denoting the amount of the available energy at the beginning of a cycle in the battery of a typical UE	—
E_h (e_h)	Random variable denoting the harvested energy in a cycle (and its mean value)	—
E_s (E_c)	Energy consumption in successful (collided) transmission	5 (3)
$N_i^r(n,k)$	See Equation (4)	To be calculated
N_{UL}	Maximum number of RAR (i.e., maximum number of successful transmissions in a RAO)	15
N	Total number of UEs	30000
N_{PTmax}	Maximum number of retransmissions	10
N_j	Total number of contending UEs in RAO j	To be calculated
$p_{ea}(r)$	Probability of energy availability for r collided access attempts and one successful transmission	To be calculated
$p_A(i)$	Packet generation probability in the ith random access opportunity	*Beta*(3,4) distribution
p_{acb}	Access barring parameter ($p_{acb} = 1$, no barring)	(0, 1)
p_j^c	Collision probability in RAO j	To be calculated
R	Number of orthogonal preambles	54
t_{rao}	Periodicity of RAOs in ms	5 ms
t_P (T_P)	Packet generation interval in ms (in RAO)	10000 ms (2000 RAOs)
t_C (T_C)	Cycle duration in ms (in RAO)	20000 ms (4000 RAOs)
t_{acb}	Mean access barring time (ms)	4000 ms (800 RAOs)
U_{acb} (U_{bo})	Uniform random variable denoting the access barring (backoff) duration	—
w_r	Waiting time for RAR	7 ms
w_{bo}	Backoff window	21 ms
x^-	$x - 1$	—
δ_i^j	$i - j$	—

A. Number of Contending UEs

Definition 1: $N_i^r(n,k)$ is defined as the number of UEs in the ith RAO that had k access attempts and n collisions prior to reaching the ith RAO, while they have started the cycle with the energy required for r collided and one successful transmissions.

According to the definition of $N_i^r(n,k)$, we recognize four possible cases for the combination of n and k as follows.

1) *$n = 0$ and $k = 0$:* This case includes the UEs with a new packet to send since they had no access attempts and no collisions before the ith RAO.
2) *$n = 0$ and $k \geq 1$:* This case includes the UEs that are still trying to get access to the PRACH (i.e., passing the ACB phase), and in the current RAO, they are doing their $k + 1$th access attempt.

3) *$n = 1$ and $k \geq 1$:* This case includes the UEs that got access to the PRACH just in their previous access attempt (i.e., kth attempt), but their transmission failed due to collision.
4) *$1 < n < N_{PTmax}$ and $k \geq 1$:* This case includes the UEs that got access in their kth access attempt and had n collisions after passing the ACB phase.

The cases mentioned above are identified based on the expressions that yield the number of the UEs in each cases. In the following, the details of these expressions are explained. Note that by separating the UEs based on their initial energy, r, we can determine how many UEs would have enough energy to still continue their contention in different RAOs of a cycle. An example of the evolution of n and k over time is presented in Fig. 3. By defining $x^- = x - 1$ and $\delta_i^j = i - j$, we have the following recursive expression for $N_i^r(n,k)$, $i = 2, 3, \ldots, T_C$

$$N_i^r(n,k) = \mathbb{1}_{r \geq n} \times \begin{cases} p_{ea}(r) N p_A(i), & n = 0,\ k = 0 \\ \sum_{j=1}^{i-1} (1 - p_{\text{acb}}) N_j^r\left(0, k^-\right) \mathbb{P}\left(U_{\text{acb}} = \delta_i^j\right), & n = 0,\ k \geq 1 \\ p_{\text{acb}} \sum_{j=1}^{i-1} N_j^r\left(0, k^-\right) p_j^c \mathbb{P}\left(U_{bo} = \delta_i^j\right), & n = 1,\ k \geq 1 \\ \sum_{j=1}^{i-1} N_j^r\left(n^-, k\right) p_j^c \mathbb{P}\left(U_{bo} = \delta_i^j\right), & 1 < n < N_{\text{PTmax}} \\ & k \geq 1 \end{cases} \tag{4}$$

with the following initial condition:

$$N_1^r(n,k) = \begin{cases} p_{ea}(r) N p_A(1), & n = 0, k = 0 \\ 0, & \text{otherwise} \end{cases} \tag{5}$$

where $\mathbb{1}$ is the indicator function, p_j^c is the collision probability in the jth RAO, and U_{acb} and U_{bo} are the PMF of access barring time and backoff period in the unit of RAO, respectively. The expressions presented in the four different branches of (4) are explained as follows.

1) In the first branch, $p_{ea}(r)$ denotes the probability of a typical UE having energy for one successful transmission and r retransmissions, while $Np_A(i)$ is the average number of UEs with fresh packet arrivals at RAO i. Hence, their product gives us the average number of fresh arrivals with sufficient energy for one successful transmission and r retransmissions.
2) In the second branch, each term inside the summation, i.e., $(1 - p_{\text{acb}}) N_j^r(0, k^-) \mathbb{P}(U_{\text{acb}} = \delta_i^j)$, is the number of UEs with $k - 1$ barred access attempts in the jth RAO [the term $N_j^r(0, k^-)$], whose kth attempt at RAO j is also unsuccessful [the term $(1 - p_{\text{acb}})$] and the ACB mechanism redirects them to RAO i [with probability $\mathbb{P}(U_{\text{acb}} = \delta_i^j)$]. The summation is over all these UEs in all RAOs before the ith RAO.
3) The third branch is similar to the second one, except that the UEs with $k - 1$ barred access attempts in the jth RAO [the term $N_j^r(0, k^-)$] obtain their first channel access at that RAO (with probability p_{acb}), which ends up in collision (with probability p_j^c), and the backoff mechanism redirects them to RAO i [with probability $\mathbb{P}(U_{bo} = \delta_i^j)$].
4) In the last branch, the term $N_j^r(n^-, k)$ denotes the number of UEs who passed the ACB phase and have $n - 1$ collisions before RAO j. In addition, their nth transmission at RAO j ends up in collision (with probability p_j^c) and the backoff mechanism redirects them to RAO i with the corresponding probability.

According to Remark 1, by setting $z_{\text{per}} = t_{\text{rao}}$, $z_{\min}$, and $z_{\max}$ as A and B in (6), the PMF of U_{acb} and U_{bo} used in (4) can be obtained, respectively,

$$A: \begin{cases} z_{\min} = \left\lceil 0.7 \frac{t_{\text{acb}}}{t_{\text{rao}}} \right\rceil \\ z_{\max} = \left\lceil 1.3 \frac{t_{\text{acb}}}{t_{\text{rao}}} \right\rceil \end{cases}, \quad B: \begin{cases} z_{\min} = \left\lceil \frac{w_r}{t_{\text{rao}}} \right\rceil \\ z_{\max} = \left\lceil \frac{w_r + w_{bo}}{t_{\text{rao}}} \right\rceil \end{cases}. \tag{6}$$

To derive the collision probability, p_j^c, it is necessary to obtain the number of contending UEs in the jth RAO. Based on Definition 1, we know that every UE with $n > 0$ have already access to the PRACH, however, UEs with $n = 0$ are still trying to pass the ACB phase. Therefore, the number of contending UEs in the jth RAO, N_j, can be derived as

$$N_j = \sum_{r=0}^{N_{\text{PTmax}}^-} \sum_{k=0}^{\infty} \left\{ N_j^r(0,k) p_{\text{acb}} + \sum_{n=1}^{N_{\text{PTmax}}^-} N_j^r(n,k) \right\}. \tag{7}$$

B. Collision and Energy State Transition Probabilities

Before presenting p_j^c, it is worth to note two important points. First, our analysis is a mean-value analysis (similar to [24]), we treat with random variables (such as number of contending UEs) as deterministic parameters that are equal to the mean value of the original random variables. For this reason, we set $p_j^c = 0$ whenever $N_j < 1$, because there is no collision when the number of contending UEs is less than one. Second, due to the limited number of access grants in an RAR, there is an upper bound on the number of UEs that receive RAR from the eNB. This upper bound is denoted by N_{UL}. Taking these two points into account, and using [24, eq. (21)], we obtain the following expression for: p_j^c, $N_j \geq 1$

$$p_j^c = 1 - \begin{cases} \left(1 - \frac{1}{R}\right)^{N_j - 1} & N_j \left(1 - \frac{1}{R}\right)^{N_j - 1} \leq N_{UL} \\ \frac{N_{UL}}{N_j}, & \text{otherwise.} \end{cases} \tag{8}$$

Note that all the listed equations depend on the energy availability probability, $p_{ea}(r)$. To obtain the value of $p_{ea}(r)$, we model the energy level in the battery of a typical UE using a Markov chain. Then, the transition probability from state E_1 to state E_2, $\mathbb{P}(E_2|E_1)$, during two consecutive cycles is given by

$$\mathbb{P}(E_2|E_1) = \mathbb{P}\left(E_{\text{cons}|E_1} = E_1 + E_h - E_2\right) \tag{9}$$

where $E_{\text{cons}|E_1}$ is a random variable denoting the energy consumption during a cycle, given that the initial energy of the UE at the beginning of the cycle is E_1. The second random variable in the transition probability presented in (9) is the harvested energy during a cycle, E_h. Using the law of total probability, we can rewrite (9) as follows:

$$\mathbb{P}(E_2|E_1) = \sum_{e=0}^{\infty} \mathbb{P}\left(E_{\text{cons}|E_1} = E_1 + e - E_2\right) \mathbb{P}(E_h = e) \tag{10}$$

where $\mathbb{P}(E_h = e)$ is the given PMF of the EH process. To obtain the PMF of $E_{\text{cons}|E_1}$, we consider all the possible values that this random variable can be taken as follows.

1) mE_c+E_s: Consumed energy when the UE has m collided access attempts before a successful access.
2) $N_{\text{PTmax}}E_c$: Consumed energy when the UE faces with transmission failure after N_{PTmax} access attempts.
3) mE_c: Consumed energy when the UE has only m retransmission opportunities during a cycle, either due to time limitation or energy limitation.

Accordingly, the PMF of $E_{\text{cons}|E_1}$ when $E_1 < E_s$, i.e., when there is no energy for even a single successful transmission is

$$\mathbb{P}\big(E_{\text{cons}|E_1} = x\big) = \begin{cases} 1 & x = 0 \\ 0 & \text{otherwise} \end{cases} \tag{11}$$

which means that no energy would be consumed in this case. For $E_1 \geq E_s$, the PMF, which covers the above-mentioned events, is equal to

$$\mathbb{P}\big(E_{\text{cons}|E_1} = x\big) = \sum_{m=0}^{N_{\text{PTmax}}} p_m^{s|r_1} I_{x=mE_c+E_s} + p^{f|r_1} I_{x=N_{\text{PTmax}}E_c} + \sum_{m=0}^{N_{\text{PTmax}}} p_m^{X|r_1} I_{x=mE_c} \tag{12}$$

where r_1 is the maximum number of retransmissions that E_1 supports, which is equal to $r_1 = \lfloor [(E_1 - E_s)/E_c] \rfloor$. The parameters $p_m^{s|r_1}$, $p^{f|r_1}$, and $p_m^{X|r_1}$ are the corresponding probabilities of the mentioned events, respectively. The parameter $p_m^{s|r_1}$ is obtained by dividing the number of UEs with m collided access attempts and one successful transmission by the number of UEs that have energy for r_1 collided attempts and one successful transmission. Hence

$$p_m^{s|r_1} = \frac{1}{p_{ea}(r_1)N} \times \begin{cases} \sum_{j=1}^{T_C} \sum_{k=0}^{\infty} N_j^{r_1}(0,k) p_{\text{acb}} \Big(1 - p_j^c\Big), & m = 0 \\ \sum_{j=1}^{T_C} \sum_{k=1}^{\infty} N_j^{r_1}(m,k) \Big(1 - p_j^c\Big), & 1 \leq m < N_{\text{PTmax}}. \end{cases} \tag{13}$$

Similarly, $p^{f|r_1}$, which is given in (14), is derived by considering the number of the UEs that had $N_{\text{PTmax}} - 1$ collided access attempts and their final attempt also leads to a collision

$$p^{f|r_1} = \frac{1}{p_{ea}(r_1)N} \sum_{j=1}^{T_C} \sum_{k=1}^{\infty} N_j^{r_1}\big(N_{\text{PTmax}}^-, k\big) p_j^c. \tag{14}$$

Finally, $p_m^{X|r_1}$ is obtained by considering two parts, First, $N_{\text{end}}^{r_1}(m,k)$, which is the number of UEs at the end of a cycle that are still trying to access the PRACH (pass the ACB phase) or trying to transmit their packets, while they have started the cycle with the energy required for r collided access attempts and one successful transmission. Second, UEs which have required energy for $m-1$ collided access attempts and one successful transmission. However, after $m-1$ collided attempts, their next attempt also leads to a collision and they face an energy depletion, before the end of the current cycle. Therefore, we have the following expression for $p_m^{X|r_1}$:

$$p_m^{X|r_1} = \frac{1}{p_{ea}(r_1)N} \times \left(\sum_{k=1}^{\infty} N_{\text{end}}^{r_1}(m,k) + \begin{cases} \sum_{j=1}^{T_C} \sum_{k=1}^{\infty} N_j^0(0,k) p_{\text{acb}} p_j^c & r_1 = 0,\ m = 1 \\ \sum_{j=1}^{T_C} \sum_{k=1}^{\infty} N_j^{r_1}\big(m^-, k\big) p_j^c & r_1 = m-1,\ m > 1 \\ 0 & \text{otherwise} \end{cases} \right). \tag{15}$$

The parameter $N_{\text{end}}^{r_1}(m,k)$, presented in (16), is obtained by simply counting the average number of UEs at the end of a cycle who had m collided access attempts and k barred attempts, with the initial energy required for r_1 collided attempts and one successful transmission

$$N_{\text{end}}^{r_1}(m,k) = \mathbb{1}_{r_1 \geq m} \times \begin{cases} (1 - p_{\text{acb}}) \sum_{j=1}^{T_C} N_j^{r_1}(0,k^-) \mathbb{P}\Big(U_{\text{acb}} > \delta_{T_C}^j\Big), & m = 0,\ k \geq 1 \\ p_{\text{acb}} \sum_{j=1}^{T_C} N_j^{r_1}(0,k^-) p_j^c \mathbb{P}\Big(U_{bo} > \delta_{T_C}^j\Big), & m = 1,\ k \geq 1 \\ \sum_{j=1}^{T_C} N_j^{r_1}\big(m^-,k\big) p_j^c \mathbb{P}\Big(U_{bo} > \delta_{T_C}^j\Big), & 1 < m < N_{\text{PTmax}} \\ & k \geq 1. \end{cases} \tag{16}$$

C. Steady-State Distribution of the Energy Levels

Having the transition probabilities in hand, we can obtain the steady-state probability distribution of the energy levels in the battery of a typical UE, i.e., $\mathbb{P}(E = x)$ and, hence, $p_{ea}(r)$ in (1). In particular, let vector $\pi_{1\times S}$ be the steady-state vector of the energy levels in the battery of a typical UE, where S is a sufficiently large constant comparing with the average energy level in the battery. Vector $\pi_{1\times S}$ is defined as follows:

$$\pi = (\mathbb{P}(E=0),\ \mathbb{P}(E=1),\ \ldots,\ \mathbb{P}(E=S-1)). \tag{17}$$

On the other hand, the one-step transition probability matrix of energy levels, $\mathbf{P}_{S\times S}$, is defined as

$$\mathbf{P} = \begin{bmatrix} \mathbb{P}(0|0) & \mathbb{P}(1|0) & \ldots & \mathbb{P}(S-1|0) \\ \mathbb{P}(0|1) & \mathbb{P}(1|1) & \ldots & \mathbb{P}(S-1|1) \\ \vdots & \vdots & \ddots & \vdots \\ \mathbb{P}(0|S-1) & \mathbb{P}(1|S-1) & \ldots & \mathbb{P}(S-1|S-1) \end{bmatrix} \tag{18}$$

where each element of $\mathbf{P}$ can be calculated using (10). According to the theory of the Markov chain, if the chain has stationary distribution, it can be calculated by solving equation $\pi\mathbf{P} = \pi$ with respect to π. Note that this is a nonlinear system of equations, since each element of $\mathbf{P}$ is also a function of π. Hence, iterative methods of solving system of nonlinear equations must be adopted to arrive at a solution. These iterative methods start from an initial point and refine the solution with a specific rule until a convergence criterion is met. We use numerical solvers (e.g., *fsolve* command in MATLAB) to solve this system of equations. The *fsolve*

command of MATLAB executes well-established algorithms, such as Levenberg–Marquardt to solve the systems composed of nonlinear equations. The stability and convergence properties of these algorithms have been investigated and confirmed in a previous publication [28]. Moreover, there are two conditions that must be satisfied to ensure that the *fsolve* command provides a valid solution. The first condition is that the input functions to the *fsolve* command are continuous and this condition is satisfied for the problem under consideration. The second condition stipulates that there is a unique solution to the problem. This condition is also satisfied based on the following two properties for the problem under consideration: 1) since every state of the Markov chain can be reached from any other state, the chain is irreducible and 2) the greatest common divisor of the required steps to return to a particular state is one, hence, the chain is aperiodic. It can thus be concluded that the chain is ergodic and the uniqueness of the steady-state distribution is guaranteed [29].

The analytical steps presented so far can be described concisely as follows. We first developed a recursive equation to obtain the number of contending UEs in each RAO. This equation can capture the effects of the time-dependent packet arrival pattern, as well as battery depletion during a cycle due to collisions. Then, the collision probability, which is a key factor for determining the number of retransmissions, was derived. However, all the results obtained depend on the distribution of the energy level in the battery of the UEs at the beginning of a cycle. We modeled the battery charge level using a Markov chain, in which the state transition probabilities were derived considering the energy consumption of UEs according to their initial energy and number of retransmissions. Steady-state distribution of this Markov chain yields the distribution of the energy level in the battery of the UEs, which completes our derivations. In fact, our model captures the interdependency between the collision probability and the battery charge level of the UEs.

D. Performance Metrics

By obtaining $p_{ea}(r)$, we can proceed further and calculate the throughput and delay. The throughput of the PRACH is defined as the ratio of the number of successful preamble transmissions during a cycle to the total number of packets in a cycle, which is equal to the total number of UEs, and can be written as follows:

$$S = \frac{1}{N}\sum_{j=1}^{T_C} N_j\left(1 - p_j^c\right). \tag{19}$$

In addition, the access delay, D, is defined as the elapsed time from the moment that a packet arrives until the UE gets access to the network. It is defined only for the UEs with successful access attempt and is the sum of the mean elapsed time in the ACB phase and backoff. UEs without collision experience only the delay that is related to the ACB phase. Hence, D, measured in seconds, is given by

$$D = \frac{t_{\text{rao}}}{S \times N}\sum_{r=0}^{N^{-}_{\text{PTmax}}}\sum_{j=1}^{T_C}\left(1 - p_j^c\right) \times \left\{ p_{\text{acb}}\sum_{k=0}^{\infty} N_j^r(0,k)k\mathbb{E}(U_{\text{acb}}) + \sum_{n=1}^{N^{-}_{\text{PTmax}}}\sum_{k=1}^{\infty} N_j^r \times (n,k)((k-1)\mathbb{E}(U_{\text{acb}}) + n\mathbb{E}(U_{bo}))\right\} \tag{20}$$

where $\mathbb{E}$ denotes the expectation operation.

The last performance metric quantifies the duration in which no packet is received from a tagged UE. This is important, especially in the M2M scenario because the UEs are supposed to report their observations in a cyclic manner and we expect the duration between two reports to be less than an application-dependent threshold. To be more specific, this metric measures the average number of cycles between two successive successful transmissions by a UE. Note that the failure in packet transmission could be due to collisions, access barring, or energy depletion. To derive this metric, we focus on the operation of the network over N_c cycles. The average number of cycles in which no packet is received from a specific UE, N_{NP}, is the summation of the cycles with unsuccessful transmissions, plus cycles with energy shortage, which is given by

$$N_{NP} = N_c\left(\sum_{r=0}^{N^{-}_{\text{PTmax}}} p_{ea}(r)\left(1 - p^{s|r}\right) + p_{eo}\right) \tag{21}$$

where $p^{s|r} = \sum_{m=0}^{r} p_m^{s|r}$ and $p_{eo} = 1 - \sum_{r=0}^{N^{-}_{\text{PTmax}}} p_{ea}(r)$. Furthermore, the average number of cycles with successful transmission, N_{ST}, is

$$N_{\text{ST}} = N_c\sum_{r=0}^{N^{-}_{\text{PTmax}}} p_{ea}(r)p^{s|r}. \tag{22}$$

The average number of cycles between two consecutive successful transmissions by a UE, N_{out}, can be obtained by dividing N_{NP} by N_{ST} and letting N_c asymptotically approach infinity as expressed by the following expression:

$$N_{\text{out}} = \lim_{N_c \to \infty}\frac{N_{NP}}{N_{\text{ST}}}. \tag{23}$$

Note that N_{out} is different from D in the way that it is computed over cycles, while D is calculated inside a cycle. In other words, D is the time duration (measured in seconds) between the generation of a packet until its successful transmission. However, N_{out} is the time duration (measured in cycles, and can be converted into seconds) between two cycles with a successful transmission from a tagged UE.

IV. Extension to Threshold-Based Activation Policy

The threshold-based activation policy is one of the common approaches in the EH communication networks to make a better use of the harvested energy [15], [19], [20]. The main idea is to let the UEs with energy less than a predefined threshold to remain silent and harvest energy for future cycles. In this section, we extend our previous results to this case in order

to investigate the joint effects of such a threshold-based activation policy with the ACB mechanism. We use the boldface notation of the parameters used in the previous section to represent them in this new scenario [e.g., $N_i^r(n,k)$ and $\boldsymbol{N}_i^r(n,k)$ for the first and second scenarios, respectively].

The details of the threshold-based activation policy are presented in the following. At each cycle, a UE starts the random access process only if it has enough energy for r_{th} failed and one successful transmission. Note that this is same as the conventional energy threshold-based activation policy, since any given energy threshold, E_{th}, can be uniquely mapped into the corresponding r_{th} using $r_{\text{th}} = \lfloor [(E_{\text{th}} - E_s)/E_c] \rfloor$. We develop our model based on r_{th}, instead of E_{th}, to facilitate the analysis. Note that the results presented in the previous section are for the special case where $r_{\text{th}} = 0$.

To investigate the effects of the presented threshold-based activation policy on our model, we revise the fundamental equation presented in (4), by replacing the term $\mathbb{1}_{r \geq n}$ with $\mathbb{1}_{r \geq \max\{n, r_{\text{th}}\}}$ to allow the UEs with sufficient energy to support at least r_{th} failed transmissions to be active. The revised version of $N_i^r(n,k)$ in (4) is denoted by $\boldsymbol{N}_i^r(n,k)$, with the following initial condition:

$$\boldsymbol{N}_1^r(n,k) = \begin{cases} \mathbb{1}_{r \geq r_{\text{th}}} \boldsymbol{p}_{ea}(r) N p_A(1), & n = 0, k = 0 \\ 0, & \text{otherwise} \end{cases} \tag{24}$$

where $\boldsymbol{p}_{ea}(r)$ is the probability of energy availability for r failed and one successful transmissions at the beginning of a cycle in the new scenario.

Using $\boldsymbol{N}_i^r(n,k)$, we can determine the number of contending UEs at RAO j, $\boldsymbol{N}_j$, and the collision probability, $\boldsymbol{p}_j^c$, in the new scenario using the same formulas presented in (7) and (8), respectively, by replacing the corresponding variables in the new scenario. We should emphasize that the first summation term in (7) is from $r = 0$ to $r = N_{\text{PTmax}}^-$, however, since $\boldsymbol{N}_i^r(n,k)$ is zero for $r < r_{\text{th}}$, the summation (7) is still applicable.

Equation (10), which determines the transition probability of the energy states of a typical UE, is quite general and apply for both scenarios, however, the value of $\mathbb{P}(E_{\text{cons}|E_1} = x)$ required to calculate the transition probabilities must be revised according to the new activation policy. We recall that in the first scenario, when $E_1 < E_s$, no energy was consumed during a cycle due to lack of sufficient energy, which led to (11). In the new scenario, we arrive at the same result (11) for the case when $E_1 < r_{\text{th}} E_c + E_s$. The rest of the equations can be used by replacing the variables in the new scenario to obtain the required performance metrics.

V. Simulation and Model Evaluation

In this section, the results of the analysis are evaluated and verified using extensive simulations. Unless otherwise specified, we use the simulation parameters that are presented in Table I. We assume that *prach-ConfigIndex* $= 6$ which results in $t_{\text{rao}} = 5$ ms. In addition, to estimate the energy consumption in the successful and failed transmissions, we use the data presented in [16, Table II]. For a failed transmission attempt, we assume approximately 1.5-mJ energy consumption, while in a successful transmission the energy consumption must be greater than 2 mJ, depending on the data packet size. Since the data packet size in the M2M scenario is small (in the order of a preamble), we use 2.5 mJ as the energy consumption in a successful transmission. On the other hand, by assuming a piezoelectric EH source, the harvested energy can be modeled by a Poisson distribution [25], i.e., $\mathbb{P}(E_h = e) = e^{-e_h}[(e_h^e)/e!]$, with a mean, e_h, depending on the size of the EH unit. For example, 500 μJ can be harvested in a second, if the harvesting unit is 10 cm^2 material [30]. Then, during a cycle with $T_c = 20$ s, 10 mJ can be harvested. Assuming 0.5 mJ as an energy unit, $E_s = 5$ and $E_c = 3$ are considered for energy consumption in successful and failed transmissions. Furthermore, with a small harvesting unit with possible energy wastage, an EH rate larger than $e_h = 1$ energy unit is reasonable to assume.

The 3GPP recommends two traffic models for the performance evaluation of M2M scenarios [23], and we use the second one, namely, Beta$(3,4)$ distribution, which is related to the heavily congested scenario. Then, the PMF of packet arrivals is given by

$$p_A(i) = \frac{60 i^2 (T_P - i)^3}{T_P^6}, \quad 1 \leq i \leq T_P$$

which is plotted in Fig. 4.

Fig. 4 shows the mean number of successful preamble transmissions ($N_j \times (1 - p_j^c)$) in different RAOs of a cycle. According to the packet arrival distribution depicted in Fig. 4, a large number of UEs generate their packet between 500th and 1000th RAO. Therefore, we observe a significant decrease in the number of successful access attempts due to collision when there is no ACB mechanism. However, after the 1000th RAO, when some of the UEs drop their packets and the packet arrival probability decreases, the success probability increases again. On the other hand, with the ACB mechanism, the number of successful attempts remains almost constant when the packet arrival probability is high (around 1000th RAO), because almost half of the UEs with new arrivals ($p_{\text{acb}} = 0.5$) postpone their transmission for a later time and the random access procedure can handle the remaining contending UEs, while it is working at its maximum capacity. In the EH cases, due to the energy outage, we see a decrease in the number of successful accesses. For example, when $e_h = 3$, the number of successful accesses in each RAO is almost half of the $e_h = \infty$ case. In fact, both the energy outage and the ACB mechanism prevent the UEs from the contention and the collision is not the cause that leads to a low success probability.

The total number of successful transmissions during a cycle, representing the network throughput, is depicted in Fig. 5 with respect to the number of UEs for different EH rates. When $e_h = \infty$, we see that in the massive M2M scenario with $N = 30\,000$, the ACB mechanism performs well with a throughput higher than 0.9, while the throughput of the legacy LTE is below 0.4. This improvement is achieved at the cost of a lower throughput for small values for N, since the ACB mechanism totally blocks the access of a small portion of UEs during a cycle, which leads to packet dropping. In addition, the ACB mechanism increases the delay. When the EH rate is low, i.e., $e_h = 1, 3$, due to the lack of energy, a large portion of the UEs are inactive, and the random access procedure can still

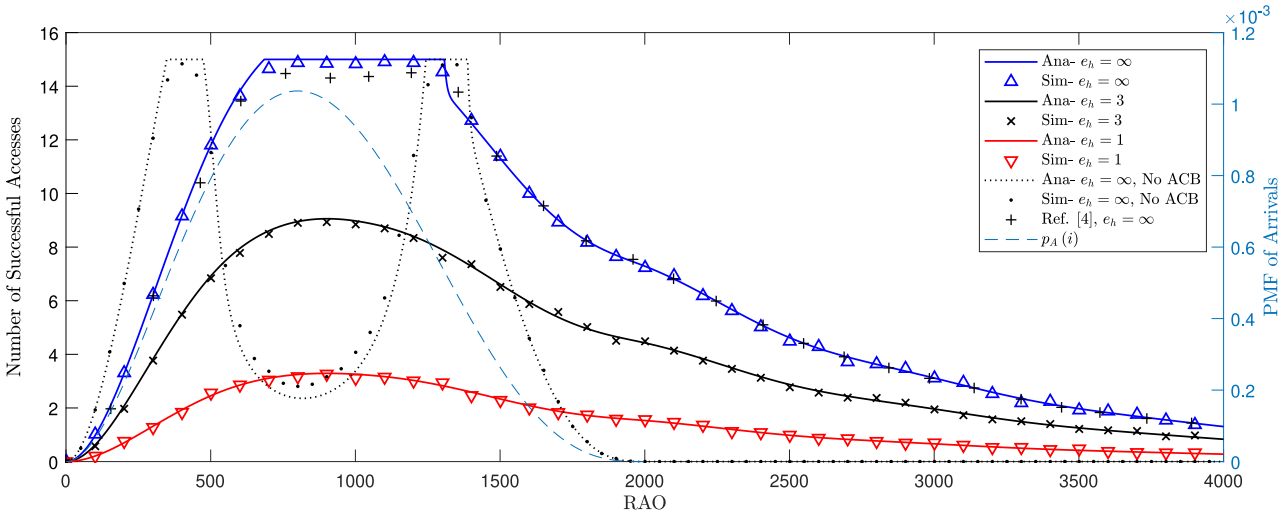

Fig. 4. Number of successful preamble transmissions in different RAOs ($p_{\text{acb}} = 0.5$ and $t_{\text{acb}} = 4$ s).

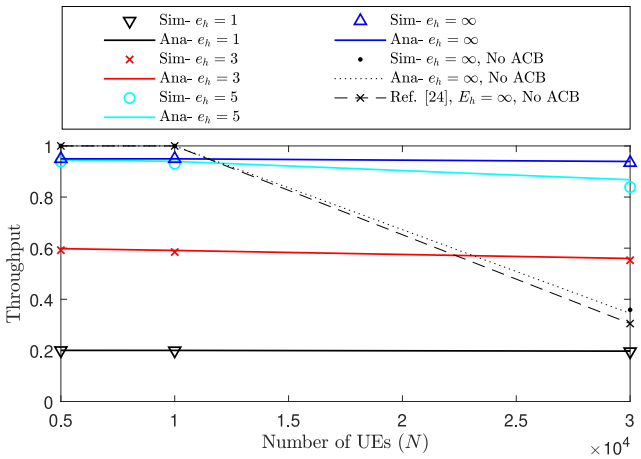

Fig. 5. Throughput with respect to the number of UEs ($p_{\text{acb}} = 0.5$ and $t_{\text{acb}} = 4$ s).

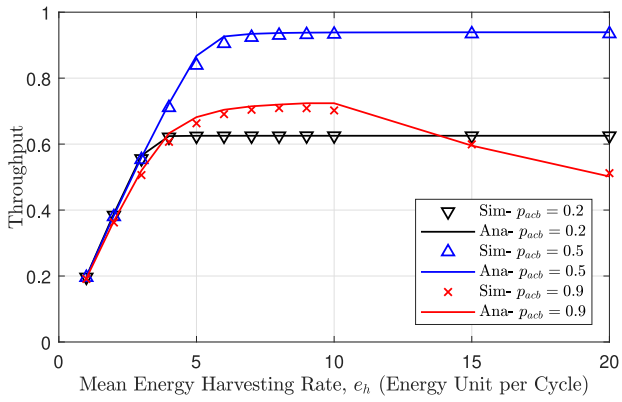

Fig. 6. Throughput of the PRACH with respect to EH rate ($t_{\text{acb}} = 4$ s).

handle the contention, regardless of the number of UEs, which leads to an almost constant function for the throughput of such cases. It is interesting to note that when the mean harvesting rate is 5, $e_h = 5$, which is equal to the required energy for one successful transmission, the throughput of the network is very similar to the case with $e_h = \infty$. This implies that the ACB mechanism can properly handle the collisions and that the wasted energy in the collisions is negligible.

Figs. 4 and 5 show a good agreement between the analytic and simulation results. For example, the mean square error (MSE) between the analytic and simulation results in Fig. 4 for $e_h = \infty$, $e_h = 3$, and $e_h = 1$ are 0.0191, 0.0108, and 0.0032, respectively, while for the No ACB case with $e_h = \infty$ MSE is 0.1155. On the other hand, the existing results in the literature for the number of successful access (the curve indicated by "Ref. [4], $e_h = \infty$, No ACB" in Fig. 4) and throughput (the curve indicated by "Ref. [24], $e_h = \infty$, No ACB" in Fig. 5) coincide with our obtained results, which confirms the validity of our simulations. In other words, in the limiting case of $e_h \to \infty$ and $p_{\text{acb}} \to 1$, we obtain the same results as [4] and [24]. However, the small discrepancy between our results and those presented in [4] and [24] is due to the perfect physical channel assumption made in this article.

Fig. 6 illustrates the variations in the throughput of the PRACH, when the mean EH rate, e_h, is increased from 1 to 20 units of energy per cycle. We see different trends in the throughput of the network, for different values of p_{acb}. For example, when there is almost no access barring (i.e., $p_{\text{acb}} = 0.9$), increasing the EH rate may result in a lower performance, due to a higher number of active UEs and higher collision probability. Therefore, it is imperative to choose the ACB parameters in accordance with the EH rate.

The average number of cycles between two consecutive transmissions by a tagged UE, which is obtained in (23) is plotted in Fig. 7 for different values of p_{acb}. When the EH rate is low, the main reason of lack of transmission is the energy outage. Therefore, the value of N_{out} is almost independent of the value of p_{acb}. By increasing the EH rate, the energy outage problem is solved, however, especially for larger values of p_{acb}, failed transmissions due to collisions play a more prominent rule to the extent that it dominates the improvement due to energy availability. For example, when the ACB mechanism is almost deactivated ($p_{\text{acb}} = 0.9$), N_{out} starts to

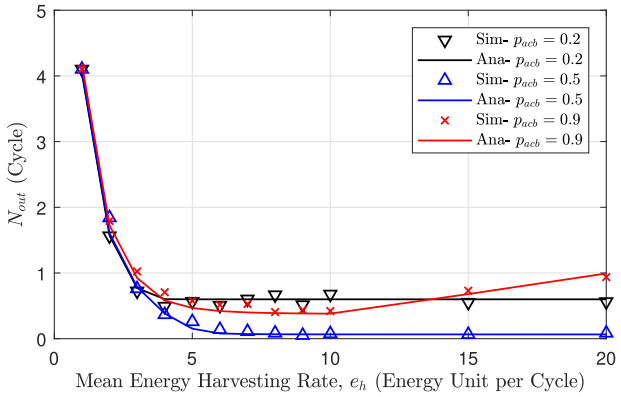

Fig. 7. Average number of cycles between two consecutive transmissions by a tagged UE with respect to EH rate.

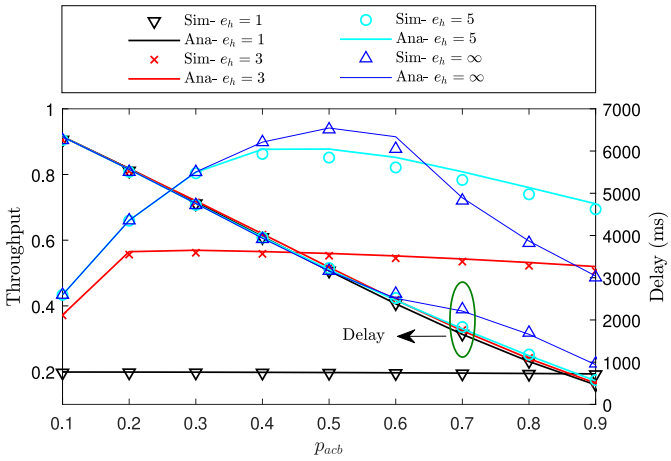

Fig. 8. Average throughput and access delay with respect to p_{acb} ($t_{\text{acb}} = 4$ s).

increase when the EH rate is high ($e_h > 10$), which is due to collisions and packet droppings.

The mean access delay of the network which is expressed in (20) is shown in Fig. 8 as a function of p_{acb}. For low values of p_{acb}, the number of the contending UEs and the resulting collision probability is very low and the delay is heavily dominated by the barring time and is almost independent of the EH rate. However, for the higher values of p_{acb}, the higher the harvesting rate is, the more intense contention. Hence, a longer delay would be experienced by successful UEs.

Fig. 8 shows the throughput that is derived in (19) as a function of p_{acb}. Since the LTE medium access protocol with the ACB scheme is based on the ALOHA protocol, we observe that the throughput of the system is similar to the throughput of the ALOHA protocol with the lower throughput in lower and higher values of p_{acb}. The reasons for these trends are that in the first case, the lower values of p_{acb} postpone the UE transmission until the next cycle, while, in the second case, excessive collisions lower the throughput. However, it is important to observe the shift of the equilibrium point, where the throughput is maximum, toward lower values of p_{acb} in the EH scenario. In the energy-limited EH scenario, higher values of p_{acb} not only cause collision but also deplete the battery of UE and prevent it from entering the contention in the next

TABLE II
OPTIMAL ACCESS BARRING RATE

	$E_c = 3,\ E_s = 5$		$E_c = 3,\ E_s = 7$	
	p_{acb}	Throughput	p_{acb}	Throughput
$e_h \to \infty$	0.5	0.9392	0.5	0.9392
$e_h = 5$	0.5	0.8676	0.3	0.6773
$e_h = 3$	0.25	0.5704	0.2	0.4191
$e_h = 1$	0.1	0.1986	0.1	0.1427

cycle. This means that in the EH scenario, the cost of collision is high and the ACB parameters must be selected in a more conservative fashion, that is, the ACB scheme must bar the UEs from transmission more often than the non-EH scenario. It is interesting to note that due to the lower number of active devices in the EH scenario, one may conclude intuitively that the ACB mechanism should provide more access opportunities to the UEs. However, the analysis and simulation results presented in this article contradict such an intuitive impression clearly.

To elaborate further on this aspect, we search for the values of the ACB parameters that will maximize the network throughput, regardless of the resulting delay. This choice is justified for many M2M applications. For example, consider the case where each M2M device is periodically monitoring an event and transmitting sensory data within a cycle, and any delay within the cycle period will be acceptable. This assumption is also consistent with the data traffic model used by the 3GPP in evaluating the M2M scenario [23]. The results are shown in Table II. The domain of the exhaustive search is limited to the defined set of values for these parameters by 3GPP. According to [31], the available sets for p_{acb} and t_{acb} are given by $\{0.05,\ 0.1, \ldots,\ 0.3,\ 0.4, \ldots,\ 0.7,\ 0.75,\ 0.8, \ldots,\ 0.95\}$ and $\{4,\ 8,\ 16, \ldots,\ 512$ s$\}$, respectively. For our setup, the optimum value of t_{acb} for all cases is 4 s. It is clear from Table II that by decreasing the amount of the harvested energy, p_{acb} must be reduced in order to limit the access of the UEs to the PRACH, which in turn limits the number of collisions. This confirms our previous conclusion on the conservative selection of the ACB parameters in the EH scenario. In addition, a higher energy cost, i.e., comparing ($E_c = 3$ and $E_s = 5$) with ($E_c = 3$ and $E_s = 7$), slightly intensifies this conservative behavior, as the optimum value of p_{acb} is less for this case, when the EH rate is $e_h = 3, 5$. However, for a very low harvesting rate, i.e., $e_h = 1$, due a to very low number of active UEs, and hence collisions, the optimum values of p_{acb} are the same for both cases.

Furthermore, the results shown in Fig. 8 illustrates the sensitivity of the throughput of the network to variations in p_{acb}. When the EH rate is relatively low ($e_h = 1$ or 3), the throughput is less sensitive to the changes in the value of p_{acb} following the point at which it reaches its maximum value. For example, in the case of $e_h = 3$, the throughput reaches its maximum value at $p_{\text{acb}} = 0.2$ and remains nearly constant or declines slightly for higher values of p_{acb}. The reason is that while increasing p_{acb} allows more UEs to enter into contention, the lack of sufficient energy limits the number of contending UEs. Therefore, the random access mechanism can handle the contention and avoid a drop in the throughput. In the network

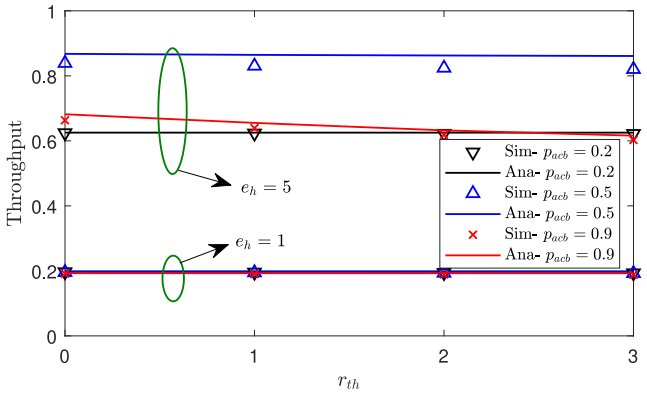

Fig. 9. Throughput as a function of r_{th}.

case without EH ($e_h = \infty$), the throughput is shown to be sensitive to variations in the value of p_{acb} and to reach its maximum value at $p_{\text{acb}} \approx 0.5$ before dropping when p_{acb} is increased as shown in Fig. 8. Thus, the selection of the value of the parameter p_{acb} has more impact on the throughput in the case without EH.

The throughput of the network as a function of retransmission threshold, r_{th}, in the threshold-based activation policy is shown in Fig. 9. Recall that, in this method, the UE is active during a cycle only if it has the required energy for at least r_{th} collisions and one successful transmission. In general, applying the threshold-based activation policy may lead to one of the following three cases.

1) *Case 1 (No Effect on the Throughput):* If collision is not a problem in the network (i.e., low collision probability), the UEs will enjoy successful transmission in their first attempt. Therefore, the energy level in the battery of the UEs oscillates around the corresponding energy threshold according to the energy consumption in each successful transmission and the amount of the harvested energy.
2) *Case 2 (Enhancing the Network Throughput):* If the energy cost of a collision is high and the network experience a high collision probability, this approach allows a subset of UEs with sufficient energy to enter the contention. Due to the lower number of contending UEs and their relatively high energy to complete enough retransmissions, the throughput of the network will be higher than in the greedy activation policy.
3) *Case 3 (Decreasing the Network Throughput):* If the energy cost of collision is low, this scheme prevents the UEs from such low-cost retries, while, in each retry, the UEs have the chance of successful transmission. This reduction in the activation probability leads to drop in the throughput.

In our considered network, the main goal of the ACB mechanism is to reduce the collisions, which means the collision problem can be solved by proper selection of the ACB parameters. On the other hand, since the LTE network uses an initial handshake before data transmission, i.e., the preamble transmission before data transmission, a collision will have a lower cost than in the conventional ALOHA-based networks. This is because a collision in the handshake phase wastes less energy than a collision in the data transmission. As a consequence, we encounter cases 1 and 3 in our network, and as can be observed from Fig. 9, the network throughput is either constant or decreasing with respect to r_{th}. We conclude that in the EH LTE network with the ACB mechanism to control collisions the threshold-based activation policy might not be as effective as in the conventional ALOHA-based networks (see [20, Fig. 6]).

VI. Conclusion

In this article, we extended the results of [24] to include the ACB mechanism and the EH capability. In particular, a recursive equation is developed to characterize the transient number of the contending UEs during a cycle in the EH-M2M LTE network under the 3GPP's ACB mechanism. The number of contending UEs depends not only on the packet arrival pattern but also on the parameters of the ACB mechanism and the amount of energy in the battery of the UEs. Using this equation and the introduced Markov chain model for the battery charge level of the UEs, we could capture the interdependency between the collision probability (and hence, the network throughput) and the energy availability in the batteries of the UEs. Based on this result, we derived the random access success probability and delay as a function of the EH rate and the ACB parameters. The results show that despite the lower number of active UEs in the EH scenario, the ACB mechanism must limit the access of these UEs to the PRACH in order to mitigate the performance degradation that results from the limited energy availability.

One natural extension to this article is to consider the non-ideal physical channel model and the advanced features in 3GPP's LTE standard such as the power ramping feature. However, we contend that this objective can be achieved, at least approximately, by properly adjusting the collision probability expressed by (8) according to the physical channel characteristics, similar to [24]. A second extension to this article is to analyze the performance of the EAB scheme of 3GPP standard in the EH scenario and compare the results with those presented in this article. Finally, the results presented in this article can be used as a foundation to analyze the performance of the random access procedure of narrow-band IoT (NB-IoT) and LTE-M standards [32], [33]. These standards have great similarities with the legacy LTE from the perspective of random access procedure. However, they deploy UE grouping based on the path loss and preamble repetition for coverage enhancement. Therefore, with proper modifications, it will be possible to apply the presented approach while including these new features.

References

[1] A. Laya, L. Alonso, and J. Alonso-Zarate, "Is the random access channel of LTE and LTE-A suitable for M2M communications? A survey of alternatives," *IEEE Commun. Surveys Tuts.*, vol. 16, no. 1, pp. 4–16, 4th Quart., 2014.
[2] *Service Accessibility, V15.2.0*, 3GPP Standard TS 22.011, Sep. 2017.

[3] L. Tello-Oquendo *et al.*, "Performance analysis and optimal access class barring parameter configuration in LTE-A networks with massive M2M traffic," *IEEE Trans. Veh. Technol.*, vol. 67, no. 4, pp. 3505–3520, Apr. 2018.

[4] I. Leyva-Mayorga, L. Tello-Oquendo, V. Pla, J. Martinez-Bauset, and V. Casares-Giner, "On the accurate performance evaluation of the LTE-A random access procedure and the access class barring scheme," *IEEE Trans. Wireless Commun.*, vol. 16, no. 12, pp. 7785–7799, Dec. 2017.

[5] R.-G. Cheng, J. Chen, D.-W. Chen, and C.-H. Wei, "Modeling and analysis of an extended access barring algorithm for machine-type communications in LTE-A networks," *IEEE Trans. Wireless Commun.*, vol. 14, no. 6, pp. 2956–2968, Jun. 2015.

[6] G.-Y. Lin, S.-R. Chang, and H.-Y. Wei, "Estimation and adaptation for bursty LTE random access," *IEEE Trans. Veh. Technol.*, vol. 65, no. 4, pp. 2560–2577, Apr. 2016.

[7] W. Zhan and L. Dai, "Throughput optimization for massive random access of M2M communications in LTE networks," in *Proc. IEEE Int. Conf. Commun. (ICC)*, Paris, France, May 2017, pp. 1–6.

[8] C.-Y. Oh, D. Hwang, and T.-J. Lee, "Joint access control and resource allocation for concurrent and massive access of M2M devices," *IEEE Trans. Wireless Commun.*, vol. 14, no. 8, pp. 4182–4192, Aug. 2015.

[9] F. Morvari and A. Ghasemi, "Two-stage resource allocation for random access M2M communications in LTE network," *IEEE Commun. Lett.*, vol. 20, no. 5, pp. 982–985, May 2016.

[10] Y. S. Reddy, A. Dubey, and A. Kumar, "A novel RACH mechanism for machine type communications in cellular networks," in *Proc. IEEE Int. Conf. Adv. Netw. Telecommun. Syst. (ANTS)*, Dec. 2017, pp. 1–6.

[11] T.-M. Lin, C.-H. Lee, J.-P. Cheng, and W.-T. Chen, "PRADA: Prioritized random access with dynamic access barring for MTC in 3GPP LTE-A networks," *IEEE Trans. Veh. Technol.*, vol. 63, no. 5, pp. 2467–2472, Jun. 2014.

[12] J. Mišić, V. B. Mišić, and N. Khan, "Sharing it my way: Efficient M2M access in LTE/LTE-A networks," *IEEE Trans. Veh. Technol.*, vol. 66, no. 1, pp. 696–709, Jan. 2017.

[13] H. Althumali and M. Othman, "A survey of random access control techniques for machine-to-machine communications in LTE/LTE-A networks," *IEEE Access*, vol. 6, pp. 74961–74983, 2018.

[14] A. Laya, L. Alonso, P. Chatzimisios, and J. Alonso-Zarate, "Massive access in the random access channel of LTE for M2M communications: An energy perspective," in *Proc. IEEE Int. Conf. Commun. Workshop (ICCW)*, London, U.K., 2015, pp. 1452–1457.

[15] M.-J. Shih, Y.-C. Pang, G.-Y. Lin, H.-Y. Wei, and R. Vannithamby, "Performance evaluation for energy-harvesting machine-type communication in LTE-A system," in *Proc. IEEE 79th Veh. Technol. Conf. (VTC Spring)*, Seoul, South Korea, May 2014, pp. 1–5.

[16] M.-J. Shih, G.-Y. Lin, and H.-Y. Wei, "Two paradigms in cellular Internet-of-Things access for energy-harvesting machine-to-machine devices: Push-based versus pull-based," *IET Wireless Sensor Syst.*, vol. 6, no. 4, pp. 121–129, 2016.

[17] Y. Liu, Z. Yang, R. Yu, Y. Xiang, and S. Xie, "An efficient MAC protocol with adaptive energy harvesting for machine-to-machine networks," *IEEE Access*, vol. 3, pp. 358–367, 2015.

[18] Z. Yang, W. Xu, Y. Pan, C. Pan, and M. Chen, "Energy efficient resource allocation in machine-to-machine communications with multiple access and energy harvesting for IoT," *IEEE Internet Things J.*, vol. 5, no. 1, pp. 229–245, Feb. 2018.

[19] F. Vázquez-Gallego, L. Alonso, and J. Alonso-Zarate, "Energy harvesting-aware distributed queuing access for wireless machine-to-machine networks," in *Proc. IEEE Glob. Commun. Conf. (GLOBECOM)*, Washington, DC, USA, Dec. 2016, pp. 1–7.

[20] F. Vázquez-Gallego, C. Kalalas, L. Alonso, and J. Alonso-Zarate, "Contention tree-based access for wireless machine-to-machine networks with energy harvesting," *IEEE Trans. Green Commun. Netw.*, vol. 1, no. 2, pp. 223–234, Jun. 2017.

[21] F. Vázquez-Gallego, J. Alonso-Zarate, and L. Alonso, "Reservation dynamic frame slotted-ALOHA for wireless M2M networks with energy harvesting," in *Proc. IEEE Int. Conf. Commun. (ICC)*, London, U.K., Jun. 2015, pp. 5985–5991.

[22] S. Wu, Y. Chen, K. K. Chai, F. Vázquez-Gallego, and J. Alonso-Zarate, "Analysis and performance evaluation of dynamic frame slotted-ALOHA in wireless machine-to-machine networks with energy harvesting," in *Proc. IEEE Globecom Workshops (GC Wkshps)*, Austin, TX, USA, Dec. 2014, pp. 1081–1086.

[23] *Study on RAN Improvements for Machine-Type Communications, V11.0.0*, 3GPP Standard TR 37.868, Sep. 2011.

[24] C.-H. Wei, G. Bianchi, and R.-G. Cheng, "Modeling and analysis of random access channels with bursty arrivals in OFDMA wireless networks," *IEEE Trans. Wireless Commun.*, vol. 14, no. 4, pp. 1940–1953, Apr. 2015.

[25] A. Tandon and M. Motani, "Diphase: Characterizing packet delay in multi-source energy harvesting systems," *IEEE Trans. Commun.*, vol. 64, no. 9, pp. 3808–3819, Sep. 2016.

[26] A. Yadav, T. M. Nguyen, and W. Ajib, "Optimal energy management in hybrid energy small cell access points," *IEEE Trans. Commun.*, vol. 64, no. 12, pp. 5334–5348, Dec. 2016.

[27] W. Liu, X. Zhou, S. Durrani, H. Mehrpouyan, and S. D. Blostein, "Energy harvesting wireless sensor networks: Delay analysis considering energy costs of sensing and transmission," *IEEE Trans. Wireless Commun.*, vol. 15, no. 7, pp. 4635–4650, Jul. 2016.

[28] N. Yamashita and M. Fukushima, "On the rate of convergence of the Levenberg–Marquardt method," in *Topics in Numerical Analysis*, G. Alefeld and X. Chen, Eds. Vienna, Austria: Springer, 2001, pp. 239–249.

[29] E. Vigoda, "Notes on Markov chains, coupling, stationary distribution," Lecture Notes CS37101, Univ. Chicago, Chicago, IL, USA, 2003.

[30] F. Mansourkiaie, L. S. Ismail, T. M. Elfouly, and M. H. Ahmed, "Maximizing lifetime in wireless sensor network for structural health monitoring with and without energy harvesting," *IEEE Access*, vol. 5, pp. 2383–2395, 2017.

[31] *Radio Resource Control (RRC); Protocol Specification, V14.4.0*, 3GPP Standard TS 36.331, Sep. 2017.

[32] Y.-P. E. Wang *et al.*, "A primer on 3GPP narrowband Internet of Things," *IEEE Commun. Mag.*, vol. 55, no. 3, pp. 117–123, Mar. 2017.

[33] A. Rico-Alvarino *et al.*, "An overview of 3GPP enhancements on machine to machine communications," *IEEE Commun. Mag.*, vol. 54, no. 6, pp. 14–21, Jun. 2016.

Sina Khoshabi Nobar received the B.S., M.S., and Ph.D. degrees in electrical engineering from the University of Tabriz, Tabriz, Iran, in 2011, 2013, and 2017, respectively.

He has been a Postdoctoral Research Fellow with Carleton University, Ottawa, ON, Canada, since 2017. His current research interests include performance analysis and optimization of wireless networks, resource allocation in cellular networks, green communication, and queuing theory.

Mohamed Hossam Ahmed (SM'07) received the Ph.D. degree in electrical engineering from Carleton University, Ottawa, ON, Canada, in 2001.

From 2001 to 2003, he was a Senior Research Associate with Carleton University. In 2003, he joined the Faculty of Engineering and Applied Science, Memorial University, St. John's, NL, Canada, where he is currently a Full Professor. He has published over 140 papers in international journals and conferences. His research is sponsored by NSERC, CFI, QNRF, Bell/Aliant, and other governmental and industrial agencies. His current research interests include radio resource management in wireless networks, multihop relaying, cooperative communication, vehicular ad hoc networks, cognitive radio networks, and wireless sensor networks.

Prof. Ahmed was a recipient of the Ontario Graduate Scholarship for Science and Technology in 1997, the Ontario Graduate Scholarship in 1998, 1999, and 2000, and the Communication and Information Technology Ontario Graduate Award in 2000. He serves as an Editor for *IEEE Communication Surveys and Tutorials*. He served as a Guest Editor of a special issue on Fairness of Radio Resource Allocation, EURASIP JWCN in 2009 and Radio Resource Management in Wireless Internet, *Wireless and Mobile Computing Journal* (Wiley, 2003). He served as the Co-Chair of the Signal Processing Track in ISSPIT'14 and Transmission Technologies Track in VTC'10-Fall, and the multimedia and signal processing symposium in CCECE'09. He is a registered Professional Engineer (P.Eng.) in the province of Newfoundland, Canada.

Yasser Morgan (M'97) received the B.Sc. and M.Sc. degrees in engineering from Cairo University, Giza, Egypt, and the Ph.D. degree from Carleton University, Ottawa, ON, Canada.

He is currently a Professor with the Faculty of Engineering and Applied Science, University of Regina, Regina, SK, Canada. In 1990, he developed a system of document scanning and document security that was adopted to protect the Canadian passport security and moved to become the standard for state travel documents. He has authored and coauthored many research papers in addition to contributions to standards, such as 3GPP, IETF, IEEE, and IEEE-SA. He founded the BRiC Laboratories, University of Regina to investigate, research, and build novel solutions for modern public safety challenges. Since its foundation, BRiC has developed further to become a major research center for advancing public safety informatics in Canada and around the world. His current research interests include wireless communications, MESH networks, mobile ad hoc networks, MAC layer and service discovery algorithms, mobile applications and middleware, distributed and pervasive computing, and public safety applications.

Prof. Morgan is also known for his contributions to the IEEE 802.11p standards group and the IEEE 1609.0/.1/.2/.3/.4/.5 WAVE groups.

Samy A. Mahmoud (M'89–SM'99–LSM'17) received the master's and Ph.D. degrees in electrical engineering from Carleton University, Ottawa, ON, Canada, in 1971 and 1975, respectively.

In 1975, he joined the Faculty of Engineering and Design, Carleton University, where he served as the Chair of the Department of Systems and Computer Engineering from 1986 to 1998 and as the Dean from 1998 to 2006. He was subsequently appointed to the position of the President and a Vice Chancellor of Carleton University from 2006 to 2008, where he is currently a Professor Emeritus. He published over 200 journals and conference papers in the fields of telecommunications, electronics, and optoelectronics and supervised 40 doctoral and 84 masters students to completion. He has coauthored of a major textbook entitled *Communication Systems Analysis and Design* (Pearson-Prentice-Hall, 2004). His current research interests include intelligent transportation systems, green communications, adaptive wireless networks, sensor networks, and autonomous vehicles.

Prof. Mahmoud was a recipient of several Canadian national awards in recognition of his original research contributions that led to technology transfer to industry. He served as a Guest Editor for two JSAC/IEEE special issues on wireless communications. He also served as a Senior Consultant to several national and international regulatory authorities and major industrial organizations in the telecommunications and spectrum management fields.